Probing Higgs boson self-interactions in proton-proton collisions at a center-of-mass energy of 100 TeV

Benjamin Fuks,[1,2,*] Jeong Han Kim,[3,4,†] and Seung J. Lee[5,6,‡]

[1]*Sorbonne Universités, UPMC Univ. Paris 06, UMR 7589, LPTHE, F-75005 Paris, France*
[2]*CNRS, UMR 7589, LPTHE, F-75005 Paris, France*
[3]*Department of Physics, Korea Advanced Institute of Science and Technology,
335 Gwahak-ro, Yuseong-gu, Daejeon 305-701, Korea*
[4]*Center for Theoretical Physics of the Universe, IBS, 34051 Daejeon, Korea and Center for Axion and
Precision Physics Research, IBS, 34141 Daejeon, Korea*
[5]*Department of Physics, Korea University, Seoul 136-713, Korea*
[6]*School of Physics, Korea Institute for Advanced Study, Seoul 130-722, Korea*

We present a phenomenological study of triple-Higgs production in which we estimate the prospects for measuring the form of the Higgs potential at future circular collider projects. We analyze proton-proton collisions at a center-of-mass energy of 100 TeV and focus on two different signatures in which the final state is made of four b jets and either a pair of photons or a pair of tau leptons. We study the resulting sensitivity on the Higgs cubic and quartic self-interactions and investigate how it depends on the b-tagging, tau-tagging and photon-resolution performances of detectors that could be designed for these future machines. We then discuss possible luminosity goals for future 100 TeV collider projects that would allow for a measurement of the Higgs potential and its possible departures from the Standard Model expectation.

I. INTRODUCTION

The discovery in 2012 [1,2] of a Higgs boson exhibiting properties similar to those expected from the Standard Model [3] has been one of the most important developments of the last decade in experimental particle physics. Theoretically, this new state completes the Standard Model framework and provides an explanation for both the spontaneous breaking of the electroweak symmetry [4–6] and the generation of the fermion masses [7]. This observation, however, only consists of the first ingredient allowing one to establish the Brout-Englert-Higgs mechanism and to fully confirm the Standard Model nature of the observed new state. Any conclusive statement indeed requires, in addition to the information currently available from experimental data, at least a more detailed knowledge of the form of the Higgs potential. Furthermore, regardless of a possible future evidence for physics beyond the Standard Model, the Higgs potential plays a key role in our understanding of the dynamics behind the electroweak symmetry breaking. In this context, multiple-Higgs-boson probes are the simplest processes that could get sensitivity to the Higgs trilinear and quartic self-interaction strengths, and thus to the form of the Higgs potential. Consequently, it will receive special attention during the next runs of the Large Hadron Collider (LHC) and will be an important topic of the physics program of any future high-energy machine that could be built within the next several years.

In the Standard Model, multiple-Higgs production at the LHC is rather suppressed [8–14]. Any precise enough direct measurement of the Higgs-boson trilinear coupling $\lambda_{hhh}^{\rm SM}$ will hence be challenging [15–17], and it will be impossible to get any information on the quartic Higgs self-interaction $\lambda_{hhhh}^{\rm SM}$ [18,19]. These two coupling strengths may, however, differ in other theoretical frameworks, so the double-Higgs production channel is expected to provide valuable information and constraints on new physics from the analysis of future collider data [10,20–39]. Nevertheless, none of the past or present machines are expected to get the chance of measuring or constraining the quartic Higgs self-coupling, so this task is left for the experimental future of our field, for which different options are being discussed today. In this work, we explore the opportunities that are inherent to a new accelerator facility aiming to collide highly energetic proton beams in the post-LHC era, and that may be built either at CERN [40] or at IHEP [41]. We hence investigate triple-Higgs production in the gluon fusion channel in proton-proton collisions at a center-of-mass energy of $\sqrt{s} = 100$ TeV and consider the huge statistics that could be offered by such machines aiming to collect several tens of ab^{-1} of data.

Once its decay is considered, a tri-Higgs-boson system can give rise to a variety of final state signatures. In terms of branching ratios, the most important channel consists of a final state made of six jets originating from the fragmentation of b quarks. Like for double-Higgs-boson production

*fuks@lpthe.jussieu.fr
†jeonghan.kim@kaist.ac.kr
‡sjjlee@korea.edu

when the two Higgs bosons further decay into a four–b-jet system, the observation of such a signal from the overwhelming background may not be possible without the use of either boosted object reconstruction techniques [25,42,43] or angular information [44]. Since this heavily depends on the detector capabilities in terms of both jet substructure identification and resolution, it is currently difficult to assess the prospects of the six − b-jet channel for pinning down a triple-Higgs-boson signal, with the detector technology to be adopted for the future proton-proton collider projects being undecided so far. For similar reasons, it will be difficult to determine how most of the subleading decay channels that involve W-boson pairs could be used for extracting information on the Higgs quartic self-coupling [45,46]. We consequently consider both a clean channel where four b jets and a pair of photons ($b\bar{b}b\bar{b}\gamma\gamma$) are issued from the Higgs decays, and a branching-ratio-enhanced decay mode where four b jets are produced in association with a pair of tau leptons ($b\bar{b}b\bar{b}\tau^+\tau^-$).

Our study is based on Monte Carlo simulations of proton-proton collisions at a center-of-mass energy of 100 TeV as they could occur in the currently studied Future Circular Collider (FCC) projects, and we generate and analyze both background and signal events. We moreover include generic reconstruction features and study the dependence of the FCC sensitivity to the Higgs quartic self-coupling in terms of different goals for the detector performances. In particular, we investigate the robustness of our findings in terms of b-tagging and tau-tagging efficiencies and mistagging rates, as well as in terms of photon reconstruction properties. We extend in this way previous studies that appeared at the time of the write-up of this paper [47,48], and we study the consequences of variations from an optimal search strategy on the FCC sensitivity to the quartic Higgs coupling.

The rest of this paper is organized as follows: In Sec. II, we discuss the theoretical framework that we have adopted in our study and present details on the Monte Carlo simulations that we have performed. Section III explores the prospects for the measurement of the Higgs potential by analyzing two signatures of a triple-Higgs signal, namely channels with a final state featuring four b jets and either a pair of photons or a pair of tau leptons. We then study the FCC sensitivity to deviations from the Standard Model in the Higgs trilinear and quartic interactions, and finally discuss our conclusions in Sec. IV, where we also investigate the FCC luminosity goals that should be aimed for in order to access the Higgs self-interactions.

II. THEORETICAL FRAMEWORK AND MONTE CARLO SIMULATION DETAILS

A. Triple-Higgs-boson production and decay

Our phenomenological analysis of the sensitivity of the FCC to triple-Higgs-boson events relies on Monte Carlo

simulations of proton-proton collisions to be produced at a center-of-mass energy of $\sqrt{s} = 100$ TeV. To this aim, we generate partonic events associated with the loop-induced $gg \to hhh$ subprocess within the MADGRAPH5_aMC@NLO framework [49] that has been recently extended to handle loop-induced processes [50]. Our theoretical model description is based on the Standard Model after having modified the Higgs potential to allow for deviations induced by new physics. We parametrize the latter in a model-independent fashion,

$$V_{\rm h} = \frac{m_h^2}{2}h^2 + (1 + \kappa_3)\lambda_{hhh}^{\rm SM}vh^3 + \frac{1}{4}(1 + \kappa_4)\lambda_{\rm hhhh}^{\rm SM}h^4,$$
(2.1)

where in our notation, h denotes the physical Higgs-boson field, v stands for its related vacuum expectation value, m_h stands for its mass, and the Standard Model self-interaction strengths are given by

$$\lambda_{hhh}^{\rm SM} = \lambda_{\rm hhhh}^{\rm SM} = \frac{m_h^2}{2v^2}.$$
(2.2)

Following the strategy of Ref. [51], we have implemented the above modifications of the scalar potential within the Standard Model implementation shipped with the FEYNRULES package [52] and made use of the NLoCT program [53] to generate a UFO library [54] containing both tree-level and loop-level information. In particular, this UFO module includes the R_2 counterterms relevant for the evaluation of the loop integrals in four dimensions, as performed in MADGRAPH5_aMC@NLO [55], which follows the Ossola-Papadopoulos-Pittau formalism [56,57].

We calculate the triple-Higgs-boson production cross section $\sigma_{\rm hhh}$ at the leading-order accuracy by convoluting the one-loop squared matrix elements generated by MADGRAPH5_aMC@NLO with the leading-order set of NNPDF 2.3 parton distribution functions [58]. We present the results in Fig. 1, where we show the variation of $\sigma_{\rm hhh}$ in the (κ_3, κ_4) plane. We first observe that $\sigma_{\rm hhh}$ is very sensitive to independent modifications of the trilinear Higgs coupling κ_3, and more specifically when κ_3 has a negative value. The dependence on the κ_4 parameter is milder, although large variations can be seen once the value of κ_3 is fixed. We will establish, in the next section, how the FCC could be sensitive to such variations and constrain the (κ_3, κ_4) parameter space.

Triple-Higgs production leads to a large class of possible final-state signatures once the Higgs-boson decays into a $b\bar{b}$ pair (with a branching ratio of 0.58), a WW^* pair (with a branching ratio of 0.22), a $\tau^+\tau^-$ pair (with a branching ratio of 0.064), a ZZ^* pair (with a branching ratio of 0.027) and into a $\gamma\gamma$ pair (with a branching ratio of 0.0023) are accounted for. The dominant channel corresponds to a final state comprised of six b jets, with an associated
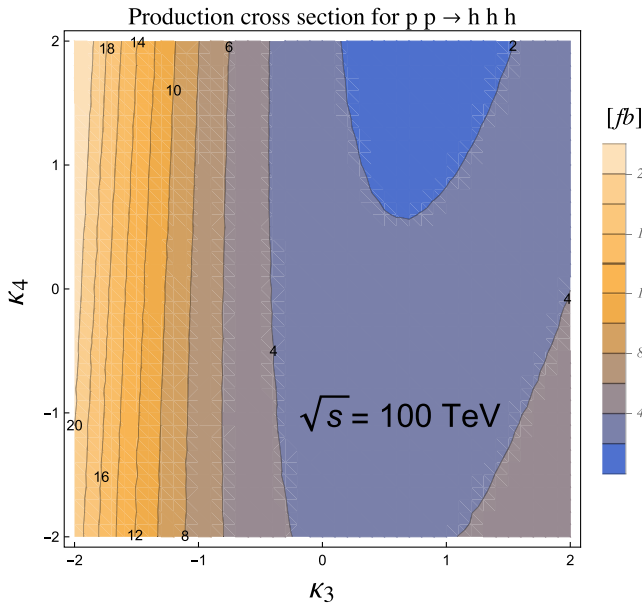
FIG. 1.   Leading-order total cross section for triple-Higgs-boson production from proton-proton collisions at $\sqrt{s} = 100$ TeV. The results are presented in terms of the κ_3 and κ_4 parameters defined in Eq. (2.1).

FIG. 2.   Relative effective resolution of the different objects used in our analysis, presented as a function of their transverse momentum.

branching ratio of 19.5%. Once a semirealistic b-tagging efficiency of 70% is included, this number drops to 14% (2.3%) when we require at least four (exactly six) b-tagged jets. The observation of such a tri-Higgs signal may, however, be complicated in particular due to the multijet background, and advanced analysis techniques may have to be used, as for the case of di-Higgs production at the LHC [25,42–44]. Such techniques are, however, strongly tied to the details of the detectors, such as tracking performance and calorimetric granularity. We therefore leave the study of this channel as an open question and focus instead on the analysis of final-state topologies that could be performed with any conceivable detector design.

The next-to-dominant channel concerns the decay of the triple-Higgs system into four b jets and a pair of W bosons, at least one of them being off shell. After imposing the semileptonic decay of the W-boson pair and including b-tagging efficiencies, the corresponding effective branching ratio reaches 1.5%. For the same reasons as those mentioned in the six − b-jet case, cornering such a triple-Higgs-boson signal within the background may require the use of techniques relying on the exact knowledge of the detector performances, as is already the case for di-Higgs production at the LHC [45,46]. We therefore ignore such a channel in our analysis, together with any other decay mode involving weak bosons.

As a consequence, we focus on the $b\bar{b}b\bar{b}\gamma\gamma$ and $b\bar{b}b\bar{b}\tau^+\tau^-$ decay channels. They feature small branching ratios of 0.232% and 6.46%, respectively, but offer good hopes to be observable even after accounting for b-tagging and tau-tagging efficiencies, in particular as the FCC
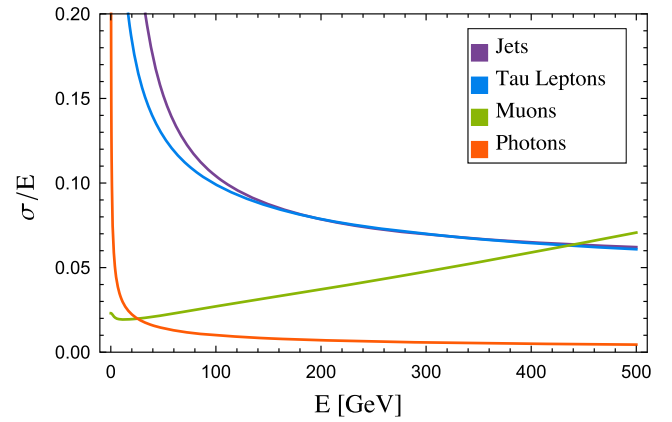
luminosity goal is of several tens of ab^{-1} [40,41]. A significant number of decayed triple-Higgs events is thus expected to be produced. As all other decay modes of the triple-Higgs-boson system imply much smaller branching ratios, they will be ignored in our analysis.

B. Event generation and analysis methods

For the simulation of the signal and background processes, we make use of the model implementation described in Sec. II A and the MADGRAPH5_aMC@NLO framework, and generate events at the leading-order accuracy in QCD. We additionally normalize all background samples by multiplying the leading-order rates by a conservative K-factor of 2. QCD corrections to the signal process, which are known to be large [12], are not included, so that the results presented below can be seen as conservative. At the generation level, we require all produced final-state particles to have a transverse momentum $p_T > 15$ GeV, to have a pseudorapidity satisfying $|\eta| < 5$, and to be separated from each other by an angular distance, in the transverse plane, of $\Delta R > 0.4$.

We perform our analysis at the partonic level, thereby neglecting the possible impact of the parton showering and the hadronization. We, however, include simplistic detector effects based on the ATLAS detector performances and smear the momentum and energy of the produced photons [59], jets and taus [60] according to the value of their transverse momentum. We summarize the p_T dependence of the resolution functions that we have employed in Fig. 2. The figure shows in particular that photons can be remarkably well reconstructed, with a relative effective resolution of $\sigma/E \sim 0.1/\sqrt{E}$ that only weakly depends on the energy. We consequently expect that the reconstruction of the Higgs mass from a diphoton system will result in a relatively narrow peak visible in the diphoton invariant-mass spectrum and centered on the true Higgs-boson mass value of 125 GeV.

Our analysis heavily relies on b-jet identification, as both considered search channels contain four (parton-level) b jets, while the investigation of the $b\bar{b}b\bar{b}\tau^+\tau^-$ channel additionally depends on the efficiency of the tau tagger. One of the aims of our study is to assess the sensitivity reach of the FCC in the (κ_3, κ_4) plane for several b-tagging and tau-tagging performances so that our results could be used as benchmarks for the FCC detector design. We consider two b-tagging setups, with an efficiency of 70%/60% for a mistagging rate of a c jet as a b jet of 18%/1.8% and of a lighter jet as a b jet of 1%/0.1% [61]. We then investigate the outcome of an optimistic tau-tagging efficiency of 80% whose associated mistagging rate of a jet as a tau is given by 0.1% [25], and also make use of a conservative tau-tagging efficiency of 50% for a fake rate of 1%.

III. PHENOMENOLOGICAL INVESTIGATIONS

We perform a study of a triple-Higgs signal produced in proton-proton collisions at a center-of-mass energy of 100 TeV and show how it can be observed above the Standard Model background in two different channels. We analyze final states comprised either of four b jets and a pair of photons (Sec. III A), or of four b jets and a pair of tau leptons (Sec. III B).

A. The $hhh \to \gamma\gamma b\bar{b}b\bar{b}$ final state

We focus first on a subprocess in which the triple-Higgs-boson system decays into four b jets and a photon pair. Our analysis strategy relies mainly on the two photons which consist of a clean probe for new physics, as it is associated with a small Standard Model background. Although the diphoton component of the final state could provide an efficient handle for background rejection and signal detection, the considered process suffers from a significant reduction of the production cross section due to the small branching fraction of a Higgs boson into a photon pair.

On the basis of the final-state topology, events are preselected by demanding that they contain at least four jets with a transverse momentum p_T and a pseudorapidity η satisfying $p_T^{j_1} > 50$ GeV, $p_T^{j_2} > 30$ GeV, $p_T^{j_3} > 20$ GeV, $p_T^{j_4} > 15$ GeV and $|\eta^{j_i}| < 2.5$ for $i = 1, 2, 3, 4$. In addition, we require the presence of two photon candidates whose transverse momentum and pseudorapidity fulfill $p_T^{\gamma_1} > 35$ GeV, $p_T^{\gamma_2} > 15$ GeV and $|\eta^{\gamma_j}| < 2.5$ for $j = 1$, 2. In order to reduce a possible signal contamination by jets misidentified as photons, we impose that the photons must be isolated in a way in which the transverse energy $E_{\mathrm{T,iso}}$ lying in a cone of radius $R_{\mathrm{iso}} = 0.3$ centered on each photon is smaller than 6 GeV [62].

We then reconstruct the two Higgs bosons originating from the four jets and impose that their invariant masses m_{jj_1} and m_{jj_2} satisfy $|m_h - m_{jj_k}| < 15$ GeV for $k = 1, 2$. In cases where there are more than one combination of dijet
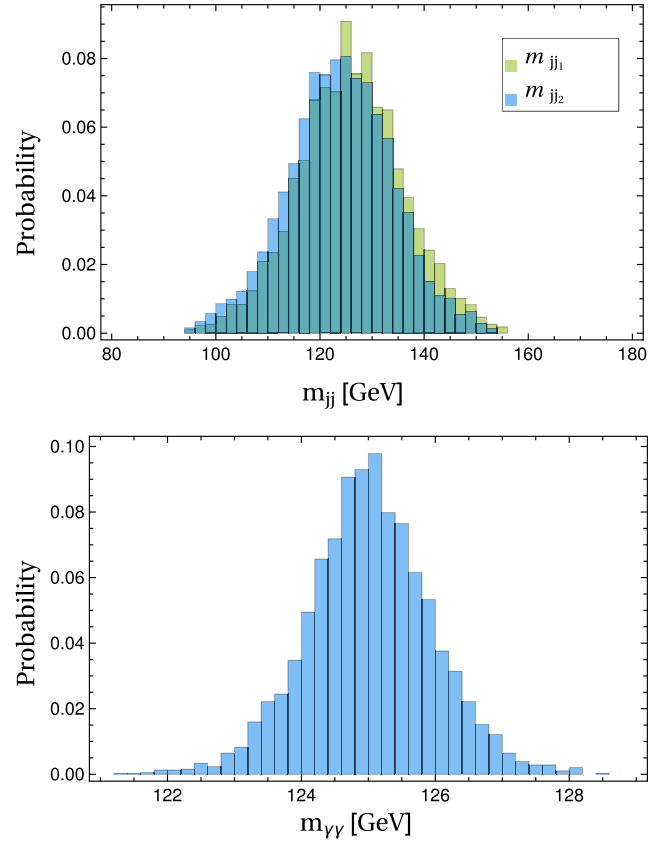

FIG. 3. Invariant-mass distributions of the three reconstructed Higgs bosons from the four final-state jets (upper panel) and two final-state photons (lower panel) after applying the preselection. We have considered a benchmark scenario in which $\kappa_3 = -2$ and $\kappa_4 = 0$.

systems compatible with this criterion, we select the one minimizing the mass asymmetry

$$\Delta_{jj_1, jj_2} = \frac{m_{jj_1} - m_{jj_2}}{m_{jj_1} + m_{jj_2}}. \qquad (3.1)$$

The remaining Higgs boson is reconstructed from the diphoton system, and we demand that its invariant mass $m_{\gamma\gamma}$ fulfill $|m_h - m_{\gamma\gamma}| < M$ where the threshold M can vary from 1 to 5 GeV. Illustrative signal distributions for a benchmark scenario in which $\kappa_3 = -2$ and $\kappa_4 = 0$ are shown in Fig. 3. The results, however, only mildly depend on the choices for the κ parameters. We therefore already conclude at that stage of our analysis that a high-quality mass resolution in the diphoton spectrum will be an incontrovertible ingredient to be able to reasonably disentangle a signal from the background. We finally require that the selected events feature at least N_b^{min} b-tagged jets with $N_b^{\mathrm{min}} = 2, 3$ or 4.

After this selection, the dominant sources of Standard Model background consist of $\gamma\gamma b\bar{b}jj$, $\gamma\gamma t\bar{t}$ (with both top quarks decaying hadronically), $\gamma\gamma Z_{bb}jj$, $h_{\gamma\gamma}h_{bb}Z_{bb}$ and
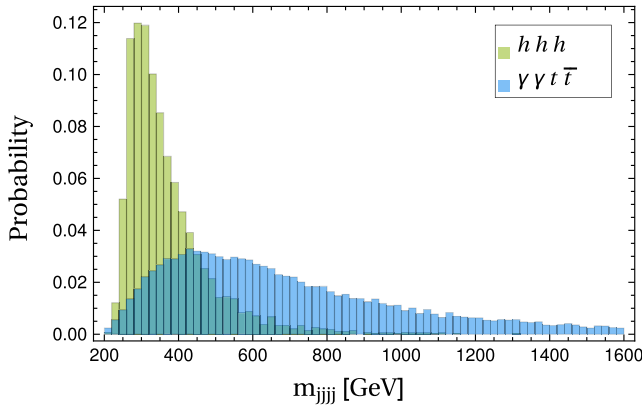
FIG. 4. Invariant-mass distributions of the four leading jets for both the triple-Higgs signal and the $t\bar{t}\gamma\gamma$ background. Event preselection has been applied, and we have considered a scenario in which $\kappa_3 = -2$ and $\kappa_4 = 0$.

$h_{\gamma\gamma}b\bar{b}b\bar{b}$ events, with h_{XX} and Z_{XX} indicating a Higgs and a Z boson decaying into an XX final state, respectively. All other Standard Model processes, including in particular $\gamma\gamma b\bar{b}b\bar{b}$ and $\gamma\gamma Z_{bb}Z_{bb}$ production, have been found to yield a negligible impact. It is further possible to reduce the $\gamma\gamma t\bar{t}$ background by constraining the invariant mass of the four-jet system m_{jjjj}. In the background case, typical m_{jjjj} values tend to be large, since the decay products of a massive top quark can acquire a significant p_T. This contrasts with the signal, as depicted in Fig. 4 for a setup in which $\kappa_3 = -2$ and $\kappa_4 = 0$. Constraining m_{jjjj} to be small could hence reduce the background and maintain a good signal efficiency. This property is further illustrated in Fig. 5, where we show the transverse-momentum spectra of the four leading jets in the signal case. The resulting invariant-mass distribution consequently peaks at a low value, since the jets have a small p_T most of the time. We have verified that this feature is independent of the values of the κ parameters, and have found that requiring $m_{jjjj} < 600$ GeV significantly reduces the $\gamma\gamma t\bar{t}$ background without affecting the signal.

The b-tagging strategy plays a central role in the possibility of observing a signal from the background. We start by making use of a conservative estimate for the b-tagging performances, and consider a tagging efficiency of 60% for mistagging rates of 1.8% and 0.1% for c and lighter jets, respectively. We present in Table I (upper table) the effects of our selection strategy for a benchmark scenario in which $\kappa_3 = -2$ and $\kappa_4 = 0$, and for a given luminosity of 20 ab^{-1}. We have varied the diphoton invariant-mass resolution M from 1 GeV to 5 GeV and the minimum number of required b-tagged jets from $N_b^{\min} = 2$ to $N_b^{\min} = 4$. We have found that for all choices of M values, a demand of at least three or four b-tagged jets is in order so that one could get some sensitivity to the signal. We have here defined the significance σ as a likelihood ratio [63],
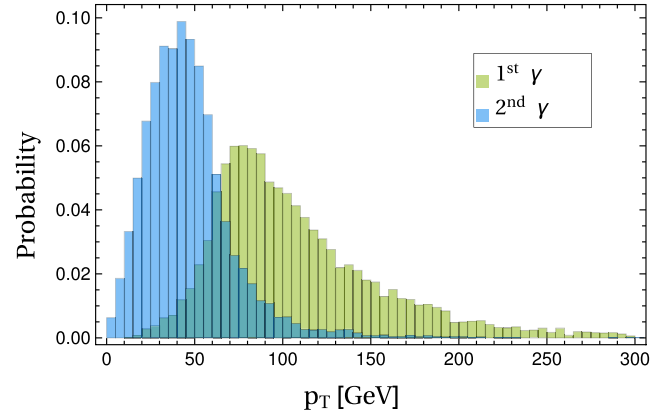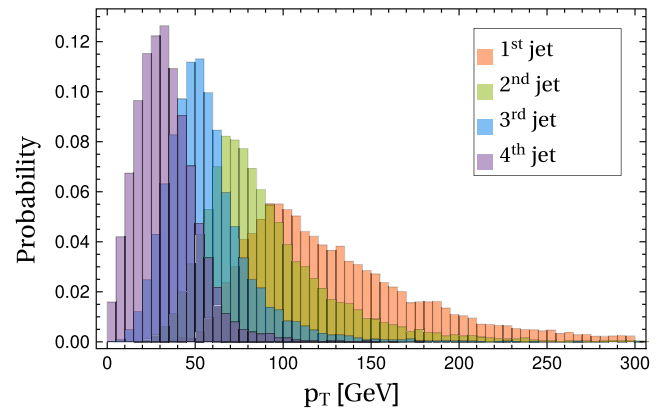

FIG. 5. Transverse-momentum distributions of the four b jets and of the two photons arising from a triple-Higgs signal before applying any event selection and for a scenario in which $\kappa_3 = -2$ and $\kappa_4 = 0$.

$$\sigma \equiv \sqrt{-2\ln\frac{L(S+B|B)}{L(B|B)}}, \qquad (3.2)$$

where S and B represent the number of selected signal and background events, respectively, and L is the likelihood function

$$L(x|n) = \frac{x^n}{n!}e^{-x}. \qquad (3.3)$$

For this very specific scenario, it is not possible to determine the diphoton mass resolution that would be necessary for observing the signal.

We have then studied the stability of these conclusions when varying both κ parameters. We have found that in general, the signal efficiency shows a strong dependence on κ_3, in particular due to the jet and photon p_T distributions that are slightly harder when κ_3 is large and positive. On the contrary, it is less sensitive to κ_4. Both these conclusions are illustrated in Fig. 6 for different configurations of the M and $N_b^{\min}$ variables of the selection strategy, and for two luminosity goals of 3 and 20 ab^{-1}.

TABLE I. Effects of our selection strategy for an illustrative benchmark scenario in which $\kappa_3 = -2$ and $\kappa_4 = 0$. We show the resulting cross sections after each of the selection steps. In the upper (lower) table, we assume a b-tagging efficiency of 60% (70%) and a mistagging rate of c and lighter jets as a b jet of 1.8% (18%) and 0.1% (1%), respectively. The significance σ is calculated for a luminosity of 20 ab^{-1}.

Selection step	Signal	$\gamma\gamma b\bar{b}jj$	$\gamma\gamma Z_{bb}jj$	$\gamma\gamma t\bar{t}$	$h_{\gamma\gamma}h_{bb}Z_{bb}$	$h_{\gamma\gamma}b\bar{b}b\bar{b}$	σ
Preselection	19 ab	4.2×10^6 ab	5.3×10^4 ab	1.1×10^5 ab	0.990 ab	7.10 ab	0.04
$|m_h - m_{jj_1,jj_2}| < 15$ GeV	14 ab	1.7×10^5 ab	1.8×10^3 ab	1.1×10^4 ab	0.059 ab	0.29 ab	0.15
$|m_h - m_{\gamma\gamma}| < 5$ GeV	14 ab	6.9×10^3 ab	68 ab	500 ab	0.058 ab	0.29 ab	0.75
$m_{jjjj} < 600$ GeV	14 ab	6.9×10^3 ab	68 ab	280 ab	0.058 ab	0.29 ab	0.72
At least 2 b-tagged jets	8.9 ab	850 ab	19 ab	47 ab	0.037 ab	0.19 ab	1.3
At least 3 b-tagged jets	6.5 ab	12 ab	0.26 ab	0.89 ab	0.027 ab	0.14 ab	6.9
At least 4 b-tagged jets	1.8 ab	9.6×10^{-3} ab	2.0×10^{-3} ab	1.9×10^{-3} ab	7.5×10^{-3} ab	0.038 ab	7.9
$|m_h - m_{\gamma\gamma}| < 2$ GeV	14 ab	2.9×10^3 ab	34 ab	210 ab	0.056 ab	0.28 ab	1.1
$m_{jjjj} < 600$ GeV	13 ab	2.9×10^3 ab	34 ab	120 ab	0.055 ab	0.28 ab	1.1
At least 2 b-tagged jets	8.6 ab	630 ab	12 ab	15 ab	0.036 ab	0.18 ab	1.5
At least 3 b-tagged jets	6.3 ab	5.6 ab	0.025 ab	0.38 ab	0.026 ab	0.13 ab	8.8
At least 4 b-tagged jets	1.7 ab	4.6×10^{-3} ab	1.2×10^{-5} ab	1.1×10^{-3} ab	7.1×10^{-3} ab	0.036 ab	7.8
$|m_h - m_{\gamma\gamma}| < 1$ GeV	11 ab	1.2×10^3 ab	34 ab	94 ab	0.041 ab	0.22 ab	1.3
$m_{jjjj} < 600$ GeV	10 ab	1.2×10^3 ab	34 ab	54 ab	0.040 ab	0.22 ab	1.3
At least 2 b-tagged jets	6.5 ab	420 ab	12 ab	12 ab	0.026 ab	0.14 ab	1.4
At least 3 b-tagged jets	4.8 ab	4.4 ab	0.025 ab	0.12 ab	0.019 ab	0.10 ab	7.7
At least 4 b-tagged jets	1.3 ab	3.9×10^{-3} ab	1.2×10^{-5} ab	4.8×10^{-4} ab	5.2×10^{-3} ab	0.029 ab	6.8

Selection step	Signal	$\gamma\gamma b\bar{b}jj$	$\gamma\gamma Z_{bb}jj$	$\gamma\gamma t\bar{t}$	$h_{\gamma\gamma}h_{bb}Z_{bb}$	$h_{\gamma\gamma}b\bar{b}b\bar{b}$	σ
Preselection	19 ab	4.2×10^6 ab	5.3×10^4 ab	1.1×10^5 ab	0.990 ab	7.10 ab	0.04
$|m_h - m_{jj_1,jj_2}| < 15$ GeV	14 ab	1.7×10^5 ab	1.8×10^3 ab	1.1×10^4 ab	0.059 ab	0.29 ab	0.15
$|m_h - m_{\gamma\gamma}| < 5$ GeV	14 ab	6.9×10^3 ab	68 ab	500 ab	0.058 ab	0.29 ab	0.75
$m_{jjjj} < 600$ GeV	14 ab	6.9×10^3 ab	68 ab	280 ab	0.058 ab	0.29 ab	0.72
At least 2 b-tagged jets	11 ab	1.3×10^3 ab	27 ab	74 ab	0.045 ab	0.23 ab	1.3
At least 3 b-tagged jets	8.9 ab	160 ab	3.5 ab	12 ab	0.038 ab	0.19 ab	2.9
At least 4 b-tagged jets	3.3 ab	1.3 ab	0.27 ab	0.26 ab	0.014 ab	0.071 ab	7.4
$|m_h - m_{\gamma\gamma}| < 2$ GeV	14 ab	2.9×10^3 ab	34 ab	210 ab	0.056 ab	0.28 ab	1.1
$m_{jjjj} < 600$ GeV	13 ab	2.9×10^3 ab	34 ab	120 ab	0.055 ab	0.28 ab	1.1
At least 2 b-tagged jets	10 ab	890 ab	17 ab	25 ab	0.043 ab	0.22 ab	1.5
At least 3 b-tagged jets	8.6 ab	76 ab	0.33 ab	5.2 ab	0.036 ab	0.18 ab	4.1
At least 4 b-tagged jets	3.2 ab	0.62 ab	1.7×10^{-3} ab	0.15 ab	0.013 ab	0.067 ab	8.6
$|m_h - m_{\gamma\gamma}| < 1$ GeV	11 ab	1.2×10^3 ab	34 ab	94 ab	0.041 ab	0.22 ab	1.3
$m_{jjjj} < 600$ GeV	10 ab	1.2×10^3 ab	34 ab	54 ab	0.040 ab	0.22 ab	1.3
At least 2 b-tagged jets	7.9 ab	590 ab	17 ab	17 ab	0.031 ab	0.17 ab	1.4
At least 3 b-tagged jets	6.6 ab	59 ab	0.33 ab	1.7 ab	0.026 ab	0.14 ab	3.6
At least 4 b-tagged jets	2.4 ab	0.54 ab	1.7×10^{-3} ab	0.065 ab	9.6×10^{-3} ab	0.053 ab	7.5

Although the constraints on the invariant mass of the three reconstructed Higgs bosons allow for a good reduction of the background, the signal stays invisible without invoking b-tagging requirements, as illustrated in Table I for a given (κ_3, κ_4) setup. Starting with a fixed value of $M = 2$ GeV ($|m_h - m_{\gamma\gamma}| < 2$ GeV) and aiming towards a luminosity of 20 ab^{-1} of proton-proton collisions at a center-of-mass energy of 100 TeV, we vary the criterion on the minimum number of b-tagged jets on the first line of Fig. 6. We do not show results for $N_b^{\min} = 2$, as this choice does not allow us to get a 2σ significance anywhere on the probed regions of the parameter space. In contrast, we present the dependence of σ for the cases in which $N_b^{\min} = 3$ (first line, left panel) and 4 (first line, right panel). We observe that a good fraction of the parameter space is covered at the 3σ level for negative κ_3 values, and that the Standard Model case of $(\kappa_3, \kappa_4) = (0, 0)$ is even almost reachable at the 3σ level for $N_b^{\min} = 4$. On the second line of the figure, we show that a lower-luminosity phase of the FCC may only be sensitive to a triple-Higgs signal for extreme deviations from the Standard Model. On the last line of Fig. 6, we fix $N_b^{\min} = 4$ and vary the value of M; i.e., the resolution on the diphoton invariant mass. We show that resolution choices of 2 GeV (first line, right figure) or
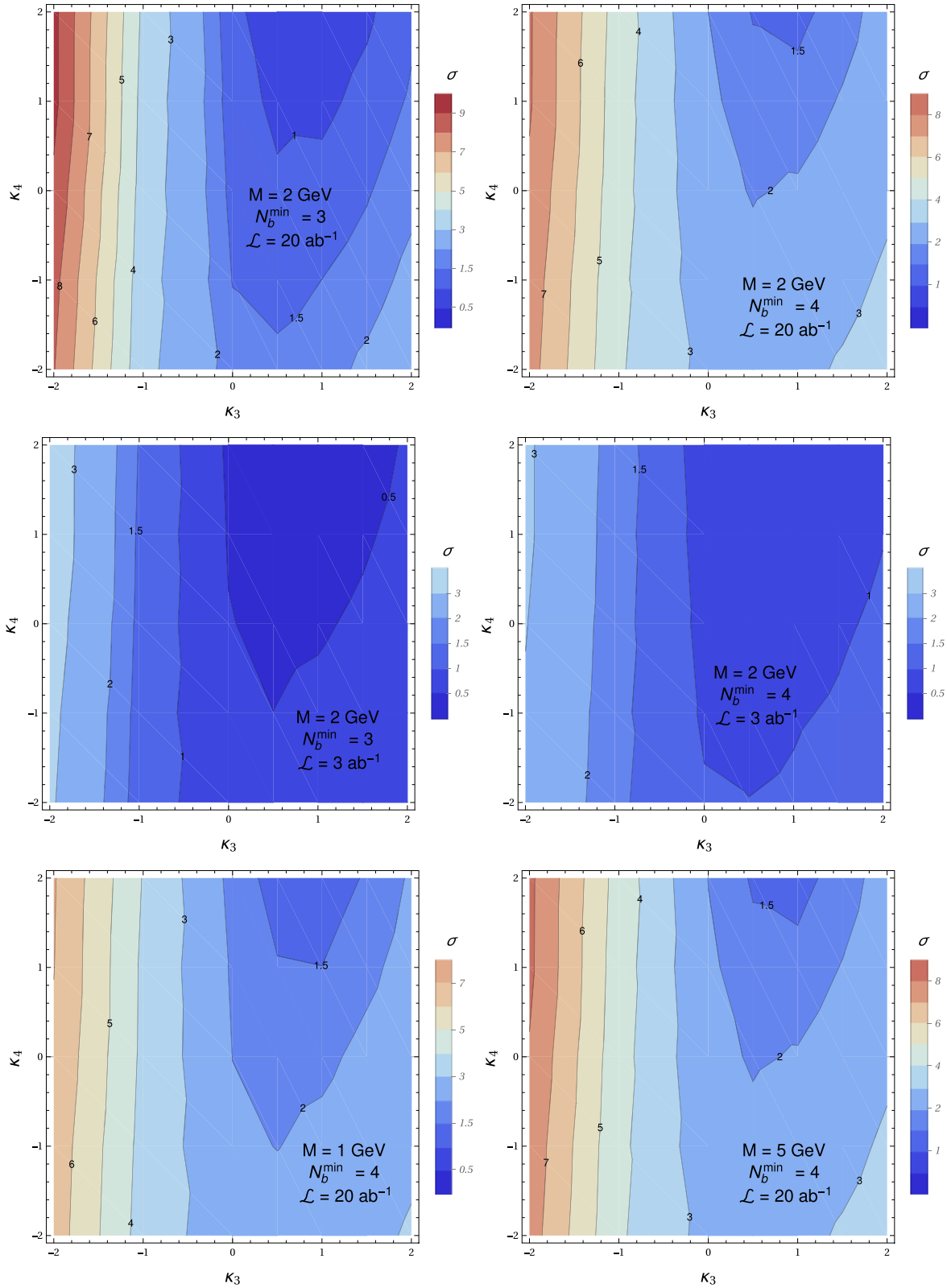
FIG. 6.   Sensitivity of the FCC to the production of a triple-Higgs system decaying into a $\gamma\gamma b\bar{b}b\bar{b}$ final state when the selection strategy depicted in the text is followed. We vary the requirement on the minimum number of b-tagged jets N_b^{min}, the diphoton mass resolution M and the luminosity $\mathcal{L}$ as indicated on the figures.

5 GeV (last line, right figure) lead to a similar sensitivity. However, adopting a resolution of 1 GeV (last line, left figure) worsens the situation due to a too low signal efficiency. It however remains to investigate how a 60% b-tagging performance could be reached at an FCC (for mistagging rates as low as 1.8% and 0.1% for c and lighter jets) and how it could be feasible to measure a diphoton invariant-mass spectrum at the 2 GeV level. Additionally, parton-shower, hadronization and underlying event effects could play a non-negligible role on photon isolation, and the contributions stemming from the multijet background could impact the significance. This has been partly studied in Ref. [47] and seems to be under good control so that all major effects are covered by the efficiency curves of Fig. 2. A complete study aiming to design an optimal analysis strategy, possibly also relying on the simulation of the pile-up, is left for future work.

In all studied setups in terms of $N_b^{\min}$, M and luminosity, we also observe that with our selection, the significance isolines follow the cross section (see Fig. 1), and that it will be challenging to get any sensitivity to the $\kappa_{3,4} > 0$ territory even during the high-luminosity phase of the FCC.

On the second panel of Table I, we investigate the effects of a more efficient b-tagging algorithm (70%) that also features larger mistagging rates of 18% and 1% for c and lighter jets. Although the signal efficiency is larger in this configuration, the background contamination is even larger, such that a poorer significance is yielded.

B. The $hhh \to \tau^+\tau^- b\bar{b}b\bar{b}$ final state

We now consider a triple-Higgs-boson signature where the final state is comprised of four b jets and a pair of hadronically decaying tau leptons. This channel has the advantage, compared to the $\gamma\gamma b\bar{b}b\bar{b}$ one, to be associated with a larger branching fraction, but it receives a more severe background contamination. As in the previous section, event preselection is performed on the basis of the final-state topology. We demand that all selected events contain at least two tagged hadronic taus whose transverse momentum $p_T^{\tau_j}$ and pseudorapidity η^{τ_j} (with $j = 1,\ 2$) satisfy $p_T^{\tau_1} > 35$ GeV, $p_T^{\tau_2} > 15$ GeV and $|\eta_{\tau_j}| < 2.5$, respectively, and four jets such that $p_T^{j_1} > 50$ GeV, $p_T^{j_2} > 30$ GeV, $p_T^{j_3} > 20$ GeV, $p_T^{j_4} > 15$ GeV and $|\eta^{j_i}| < 2.5$ for $i = 1, 2, 3, 4$.

We then reconstruct two Higgs bosons out of four (possibly fake) b jets using the method that has been introduced in Sec. III A, and require that the two reconstructed invariant masses m_{jj_k} be compatible with the Higgs-boson mass, $|m_h - m_{jj_k}| < 15$ GeV for $k = 1, 2$. We additionally impose a constraint on the third reconstructed Higgs boson by asking the di-tau invariant mass $m_{\tau\tau}$ to lie in a 10 GeV window centered on the Higgs mass. As illustrated in Fig. 7 for a scenario in which $\kappa_3 = -2$ and
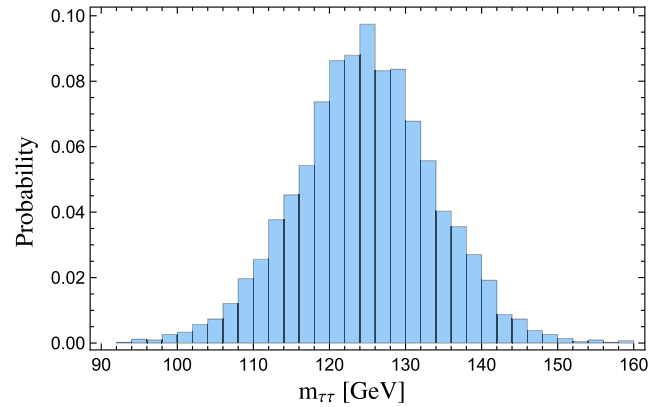

FIG. 7. Invariant-mass distribution of the Higgs boson that has been reconstructed from the di-tau system, after applying the preselection strategy. We have considered a benchmark scenario in which $\kappa_3 = -2$ and $\kappa_4 = 0$.

$\kappa_4 = 0$, this last requirement allows for the selection of a significant fraction of the signal events.

After additionally demanding that the selected events contain at least $N_b^{\min}$ b jets with $N_b^{\min} = 3$ or 4,[1] the Standard Model background turns out to be dominated by $\tau\tau t\bar{t}$ events where both top quarks decay hadronically and di-tau–plus–jet events where at least two jets are b-tagged. Moreover, $t\bar{t}h$ and $W^+W^- b\bar{b}b\bar{b}$ production also contribute significantly, the tau leptons originating here from top-quark and W-boson decays, respectively. We finally ignore QCD multijet background contributions from our analysis, as they are made negligible after fixing $N_b^{\min}$ to either 3 or 4. The corresponding rejection factor, obtained from parton-level simulations, is indeed of $10^{10} - 10^{12}$. A more precise estimate, however, necessitates to include QCD effects such as parton showers and hadronization, and pileup. This is left for future work, and we expect, as in the $\gamma\gamma b\bar{b}b\bar{b}$ case, that the bulk of the effects is covered by our mistagging rate parameterization and resolution functions.

In Table II, we present the impact of our selection, for several b-tagging and tau-tagging performances, on both the different components of the background and the signal. For the latter, we consider a benchmark scenario in which $\kappa_3 = -2$ and $\kappa_4 = 0$, and the FCC sensitivity has been calculated assuming an integrated luminosity of 20 ab^{-1} and as in Eq. (3.2). We observe that increasing the minimum number of demanded b-tagged jets to $N_b^{\min} = 4$ worsens the significance σ, as the gain in the background rejection is accompanied with an important suppression of the signal. This is further depicted in Fig. 8, where we show the dependence of the significance on the κ_3 and κ_4 parameters when at least three (left panel) and four (right panel) b-tags are requested, for a b-tagging efficiency of

---

[1]We have verified that fixing $N_b^{\min}$ to 2 was not allowing us to get any sensitivity to a triple-Higgs signal.

TABLE II.   Effects of our selection strategy for an illustrative benchmark scenario in which $\kappa_3 = -2$ and $\kappa_4 = 0$. We show the resulting background and signal cross sections after each of the selection steps, together with the related significance that has been calculated for a luminosity of 20 ab^{-1}. In the upper (lower) table, we assume a tau-tagging efficiency of 80% (50%) and a mistagging rate of jets as taus of 0.1% (1%).

Selection step	Signal	$\tau\tau b\bar{b}jj$	$\tau\tau b\bar{b}b\bar{b}$	$\tau\tau Z_{bb}jj$	$\tau\tau Z_{bb}bb$	$\tau\tau t\bar{t}$	$t\bar{t}h$	$t\bar{t}z$	$W^+W^-b\bar{b}b\bar{b}$	σ
Preselection	165 ab	1.2×10^7 ab	5.7×10^4 ab	7.4×10^4 ab	2.8×10^3 ab	2.1×10^5 ab	7.5×10^4 ab	1.0×10^4 ab	4.1×10^5 ab	0.21
$|m_h-m_{jj_1,jj_2}|<15\text{GeV}$	125 ab	4.2×10^5 ab	2.3×10^3 ab	2.8×10^3 ab	120 ab	2.8×10^4 ab	9.5×10^3 ab	300 ab	1.7×10^4 ab	0.81
$|m_h-m_{\tau\tau}|<10\text{GeV}$	94 ab	3.5×10^3 ab	31 ab	100 ab	7.9 ab	1.2×10^4 ab	900 ab	22 ab	1.2×10^3 ab	3.15
$N_b^{\min}=3(\epsilon_b=0.7)$	61 ab	35 ab	20 ab	1.0 ab	5.1 ab	520 ab	590 ab	14 ab	770 ab	6.1
$N_b^{\min}=3(\epsilon_b=0.6)$	45 ab	2.6 ab	15 ab	0.074 ab	3.7 ab	38 ab	430 ab	11 ab	560 ab	6.0
$N_b^{\min}=4(\epsilon_b=0.7)$	23 ab	0.17 ab	7.5 ab	5.0×10^{-3} ab	1.9 ab	14 ab	220 ab	5.3 ab	280 ab	4.3
$N_b^{\min}=4(\epsilon_b=0.6)$	12 ab	1.3×10^{-3} ab	4.1 ab	3.7×10^{-5} ab	1.0 ab	0.11 ab	120 ab	2.9 ab	150 ab	3.2

Selection step	Signal	$\tau\tau b\bar{b}jj$	$\tau\tau b\bar{b}b\bar{b}$	$\tau\tau Z_{bb}jj$	$\tau\tau Z_{bb}bb$	$\tau\tau t\bar{t}$	$t\bar{t}h$	$t\bar{t}z$	$W^+W^-b\bar{b}b\bar{b}$	σ
Preselection	68 ab	5.0×10^6 ab	2.4×10^4 ab	3.1×10^4 ab	1.2×10^3 ab	9.2×10^4 ab	3.1×10^4 ab	4.3×10^3 ab	1.7×10^5 ab	0.13
$|m_h-m_{jj_1,jj_2}|<15\text{GeV}$	52 ab	1.7×10^5 ab	970 ab	1.2×10^3 ab	48 ab	1.2×10^4 ab	3.9×10^3 ab	130 ab	7.0×10^3 ab	0.52
$|m_h-m_{\tau\tau}|<10\text{GeV}$	39 ab	1.5×10^3 ab	13 ab	43 ab	3.3 ab	5.1×10^3 ab	370 ab	9.1 ab	490 ab	2.0
$N_b^{\min}=3(\epsilon_b=0.7)$	25 ab	14 ab	8.6 ab	0.42 ab	2.1 ab	230 ab	240 ab	6.0 ab	320 ab	3.9
$N_b^{\min}=3(\epsilon_b=0.6)$	18 ab	1.0 ab	6.3 ab	0.031 ab	1.5 ab	16 ab	180 ab	4.3 ab	230 ab	3.9
$N_b^{\min}=4(\epsilon_b=0.7)$	9.3 ab	0.071 ab	3.2 ab	2.1×10^{-3} ab	0.78 ab	6.3 ab	90 ab	2.2 ab	120 ab	2.8
$N_b^{\min}=4(\epsilon_b=0.6)$	5.0 ab	5.2×10^{-4} ab	1.7 ab	1.5×10^{-5} ab	0.42 ab	0.046 ab	48 ab	1.2 ab	63 ab	2.1

$\epsilon_b = 70\%$ and a mistagging rate of c jets and lighter jets as b jets of 18% and 1%, respectively. Contrary to what has been found in the diphoton–plus–four-b-jet study of Sec. III A, the nature of the main background contributions is such that using a less efficient b-tagging algorithm with a smaller fake rate is reducing the triple-Higgs sensitivity.

In the lower panel of the table, we present results in which the tau-tagger performances are more conservative, with a tagging efficiency of 50% for a fake rate of 1%, and show that for the benchmark scenario under consideration, one obtains a considerable reduction of the significance. This feature holds over the entire parameter space so that the possibility of using the di-tau–plus–four-b-jet triple-Higgs channel strongly relies on the availability of an extremely good tau tagger.

IV. DISCUSSION AND FCC DESIGN CONSIDERATIONS

The form of the Higgs potential V_h belongs to the untested parts of the Standard Model Lagrangian, and it must hence be experimentally probed in the future to fully unravel the nature of the electroweak-symmetry-breaking mechanism. While in the Standard Model, all the parameters driving the bilinear, trilinear and quartic terms of V_h can be fully deduced from the measurement of the
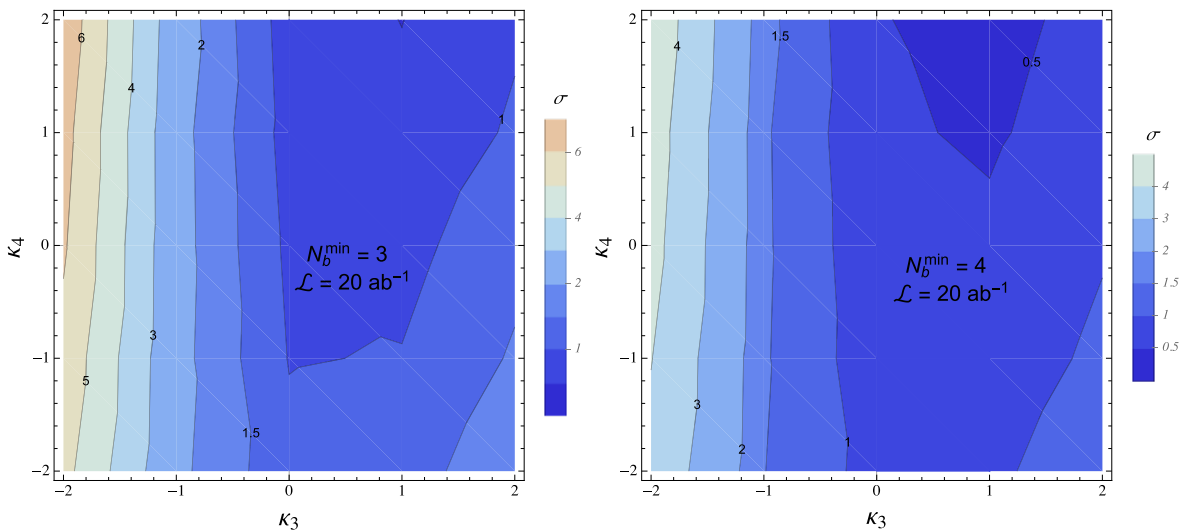

FIG. 8.   Sensitivity of the FCC to the production of a triple-Higgs system decaying into a $\tau^+\tau^-b\bar{b}b\bar{b}$ final state when the selection strategy depicted in the text is followed. We show results for $N_b^{\min}=3$ (left) and 4 (right).

Higgs-boson mass and the value of the vacuum expectation value of the Higgs field (that is determined from the W-boson mass measurement), direct and independent measurements of all of these parameters can only be achieved with the study of multiple-Higgs-boson production. The prospects for double-Higgs production, which is sensitive to the trilinear Higgs self-coupling, have been relatively well studied in the context of both the high-luminosity run of the LHC and the future colliders [8–10,12–38]. Although the knowledge of the trilinear Higgs self-coupling is not enough to fully test the Standard Model nature of the Higgs potential, triple-Higgs-boson production that is sensitive to both the trilinear and quartic Higgs self-couplings, remains less explored so far [47,48].

In this paper, we have continued to fill this gap and studied the prospects for measuring all renormalizable interaction strengths of the Higgs potential at a future proton-proton collider running at a center-of-mass energy of 100 TeV. We have focused on the production of a triple-Higgs-boson system and examined two of its specific signatures. More precisely, we have considered final states comprised of four b jets, and either a pair of photons or a pair of tau leptons. We have furthermore decided to be agnostic of any specific assumption on the future collider detector capacities and provided instead guidelines for detector designs that would allow for the observation of a triple-Higgs signal. For the same reason, the investigation of channels that are associated with large branching fractions, such as the six-b-jet or the four-b-jet–plus–W-boson-pair modes, but whose analysis requires a deeper knowledge of the FCC detector performances, has been left for a future work.

Our study indicates that triple-Higgs production is more sensitive to new physics contributions to the trilinear Higgs self-coupling (collected under the κ_3 parameter in our theoretical model description) than to the quartic one (collected under the κ_4 parameter). These findings closely follow the dependence of the triple-Higgs total cross section on the κ_i parameters so that the sensitivity reach of the FCC in the (κ_3, κ_4) plane mostly extends to regions in which the trilinear coupling is large and negative. This conclusion holds for any value of κ_4. In order to assess how the FCC would be sensitive to deviations from the Standard Model in the Higgs self-interactions and to make our results useful for detector design studies, we have made use of Monte Carlo simulations of both the signal and the Standard Model background. We have additionally explored the impact of different b-tagging and tau-tagging performances, as well as that of different diphoton invariant-mass resolutions.

We have chosen two b-tagging setups with efficiencies of 70% and 60%, respectively, for related mistagging rates of a c jet (light jet) as a b jet of 18% (1%) and 1.8% (0.1%). We have found that the best expectation is obtained by requiring at least three b-tagged jets ($N_b^{\min} = 3$) in the $\tau^+\tau^- b\bar{b}b\bar{b}$ mode and four b-tagged jets ($N_b^{\min} = 4$) in the $\gamma\gamma b\bar{b}b\bar{b}$ mode. These choices indeed allow both for an efficient background

rejection and to maintain a high signal efficiency (at the 50% level). Due to the different natures of the dominant components of the background and the b-tagging requirements of both analysis strategies, the four-b-jet–plus–diphoton study has been found to exhibit better results with a small fake rate (at the price of a smaller b-tagging efficiency), which contrasts with the four-b-jet–plus–di-tau channel, for which it is better to make use of a more efficient b-tagging algorithm (exhibiting thus a larger fake rate). We have adopted two benchmark tau-tagging performance setups. The first one is optimistic and features a tagging efficiency of 80% for an associated mistagging rate of a jet as a tau of 0.1%. The second setup is more conservative, the tagging efficiency being 50% and the fake rate 1%. We have found that only a very efficient tau-tagging algorithm provides hopes for the four-b-jet–plus–tau-pair channel to be sensitive to a triple-Higgs-boson signal. In this case, this channel can be almost as competitive, and thus complementary, to the four-b-jet–plus–two-photon channel. Nevertheless, such optimistic tau-tagging performances certainly need to be assessed by an experimental study, while our work warrants some benefits for improved tau tagging at future colliders. We have finally investigated the effects of different diphoton mass resolutions for the four-b-jet–plus–photon-pair channel, imposing the reconstructed Higgs-boson mass from the diphoton system to be compatible with the true Higgs mass at the 1, 2 and 5 GeV level. For the first choice ($|m_h - m_{\gamma\gamma}| < 1$ GeV), we have observed that the related reduced signal efficiency was worsening the FCC sensitivity to the triple-Higgs signal, while the two other cases are implying improved results, with a smaller mass resolution being preferred.

All our results mainly rely on a 20 ab^{-1} FCC luminosity (unless stated otherwise). We have, however, studied departures from this choice in order to get a useful ground for estimating luminosity goals of a future 100 TeV hadron colliders that would allow for the measurement of the quartic Higgs self-coupling. Focusing on the most
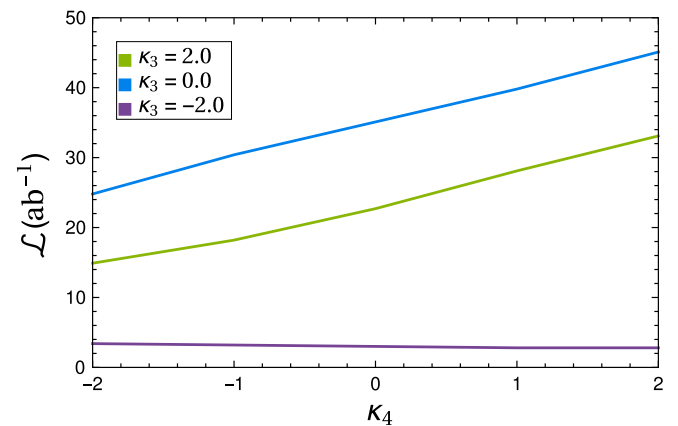

FIG. 9. Minimum FCC luminosities that are required to achieve a 3σ sensitivity to a triple-Higgs signal in terms of the κ_4 parameter for fixed values of κ_3.

promising analysis strategy in which the $\gamma\gamma b\bar{b}b\bar{b}$ channel is used with a diphoton invariant mass requirement of $|m_h - m_{\gamma\gamma}| < 2$ GeV and a demand of at least four b-tagged jets, we show in Fig. 9 the minimum FCC luminosities that would be required to achieve a 3σ sensitivity in terms of the value of the κ_4 parameter and for several fixed values of κ_3. As very large and negative κ_3 values ensure an important enhancement of the triple-Higgs production cross section, a 3σ observation of a triple-Higgs signal is guaranteed with a few ab^{-1} regardless of the size of the new physics contributions to the Higgs quartic coupling. For larger values of κ_3, a few tens of ab^{-1} (which roughly corresponds to a period of 20–30 years of FCC running [40,41]) are required, so that one will get sensitivity to only a fraction of the scanned region of the (κ_3, κ_4) parameter space.

[1] G. Aad *et al.* (ATLAS Collaboration), Phys. Lett. B **716**, 1 (2012).

[2] S. Chatrchyan *et al.* (CMS Collaboration), Phys. Lett. B **716**, 30 (2012).

[3] ATLAS and CMS Collaborations, Reports No. ATLAS-CONF-2015-044, No. CMS-HIG-15-002, 2015.

[4] F. Englert and R. Brout, Phys. Rev. Lett. **13**, 321 (1964).

[5] P. W. Higgs, Phys. Rev. Lett. **13**, 508 (1964).

[6] G. S. Guralnik, C. R. Hagen, and T. W. B. Kibble, Phys. Rev. Lett. **13**, 585 (1964).

[7] S. Weinberg, Phys. Rev. Lett. **19**, 1264 (1967).

[8] E. W. N. Glover and J. J. van der Bij, Nucl. Phys. **B309**, 282 (1988).

[9] T. Plehn, M. Spira, and P. M. Zerwas, Nucl. Phys. **B479**, 46 (1996); **B531**, 655(E) (1998).

[10] S. Dawson, S. Dittmaier, and M. Spira, Phys. Rev. D **58**, 115012 (1998).

[11] R. Frederix, S. Frixione, V. Hirschi, F. Maltoni, O. Mattelaer, P. Torrielli, E. Vryonidou, and M. Zaro, Phys. Lett. B **732**, 142 (2014).

[12] F. Maltoni, E. Vryonidou, and M. Zaro, J. High Energy Phys. 11 (2014) 079.

[13] D. de Florian and J. Mazzitelli, J. High Energy Phys. 09 (2015) 053.

[14] J. Grigo, J. Hoff, and M. Steinhauser, Nucl. Phys. **B900**, 412 (2015).

[15] U. Baur, T. Plehn, and D. L. Rainwater, Phys. Rev. Lett. **89**, 151801 (2002).

[16] U. Baur, T. Plehn, and D. L. Rainwater, Phys. Rev. D **68**, 033001 (2003).

[17] U. Baur, T. Plehn, and D. L. Rainwater, Phys. Rev. D **69**, 053004 (2004).

[18] T. Plehn and M. Rauch, Phys. Rev. D **72**, 053008 (2005).

[19] T. Binoth, S. Karg, N. Kauer, and R. Ruckl, Phys. Rev. D **74**, 113008 (2006).

[20] A. Pierce, J. Thaler, and L.-T. Wang, J. High Energy Phys. 05 (2007) 070.

[21] A. Arhrib, R. Benbrik, C.-H. Chen, R. Guedes, and R. Santos, J. High Energy Phys. 08 (2009) 035.

[22] E. Asakawa, D. Harada, S. Kanemura, Y. Okada, and K. Tsumura, Phys. Rev. D **82**, 115002 (2010).

[23] R. Grober and M. Muhlleitner, J. High Energy Phys. 06 (2011) 020.

[24] R. Contino, M. Ghezzi, M. Moretti, G. Panico, F. Piccinini, and A. Wulzer, J. High Energy Phys. 08 (2012) 154.

[25] M. J. Dolan, C. Englert, and M. Spannowsky, J. High Energy Phys. 10 (2012) 112.

[26] M. Gillioz, R. Grober, C. Grojean, M. Muhlleitner, and E. Salvioni, J. High Energy Phys. 10 (2012) 004.

[27] J. Cao, Z. Heng, L. Shang, P. Wan, and J. M. Yang, J. High Energy Phys. 04 (2013) 134.

[28] D. T. Nhung, M. Muhlleitner, J. Streicher, and K. Walz, J. High Energy Phys. 11 (2013) 181.

[29] U. Ellwanger, J. High Energy Phys. 08 (2013) 077.

[30] J. Liu, X.-P. Wang, and S.-h. Zhu, arXiv:1310.3634.

[31] J. M. No and M. Ramsey-Musolf, Phys. Rev. D **89**, 095031 (2014).

[32] J. Baglio, A. Djouadi, R. Gröber, M. M. Mühlleitner, J. Quevillon, and M. Spira, J. High Energy Phys. 04 (2013) 151.

[33] D. Y. Shao, C. S. Li, H. T. Li, and J. Wang, J. High Energy Phys. 07 (2013) 169.

[34] J. Baglio, O. Eberhardt, U. Nierste, and M. Wiebusch, Phys. Rev. D **90**, 015008 (2014).

[35] B. Hespel, D. Lopez-Val, and E. Vryonidou, J. High Energy Phys. 09 (2014) 124.

[36] C.-R. Chen and I. Low, Phys. Rev. D **90**, 013018 (2014).

[37] B. Bhattacherjee and A. Choudhury, Phys. Rev. D **91**, 073015 (2015).

[38] S. Dawson, A. Ismail, and I. Low, Phys. Rev. D **91**, 115008 (2015).

[39] R. Grober, M. Muhlleitner, M. Spira, and J. Streicher, J. High Energy Phys. 09 (2015) 092.

[40] https://fcc.web.cern.ch/Pages/Hadron-Collider.aspx.

[41] https://http://indico.ihep.ac.cn/event/3813.

[42] B. Cooper, N. Konstantinidis, L. Lambourne, and D. Wardrope, Phys. Rev. D **88**, 114005 (2013).

[43] D. E. Ferreira de Lima, A. Papaefstathiou, and M. Spannowsky, J. High Energy Phys. 08 (2014) 030.

[44] D. Wardrope, E. Jansen, N. Konstantinidis, B. Cooper, R. Falla, and N. Norjoharuddeen, Eur. Phys. J. C **75**, 219 (2015).

[45] A. Papaefstathiou, L. L. Yang, and J. Zurita, Phys. Rev. D **87**, 011301 (2013).

[46] V. Martin Lozano, J. M. Moreno, and C. B. Park, J. High Energy Phys. 08 (2015) 004.

[47] A. Papaefstathiou and K. Sakurai, J. High Energy Phys. 02 (2016) 006.

[48] C.-Y. Chen, Q.-S. Yan, X. Zhao, Y.-M. Zhong, and Z. Zhao, Phys. Rev. D **93**, 013007 (2016).

[49] J. Alwall, R. Frederix, S. Frixione, V. Hirschi, F. Maltoni, O. Mattelaer, H. S. Shao, T. Stelzer, P. Torrielli, and M. Zaro, J. High Energy Phys. 07 (2014) 079.

[50] V. Hirschi and O. Mattelaer, J. High Energy Phys. 10 (2015) 146.

[51] N. D. Christensen, P. de Aquino, C. Degrande, C. Duhr, B. Fuks, M. Herquet, F. Maltoni, and S. Schumann, Eur. Phys. J. C **71**, 1541 (2011).

[52] A. Alloul, N. D. Christensen, C. Degrande, C. Duhr, and B. Fuks, Comput. Phys. Commun. **185**, 2250 (2014).

[53] C. Degrande, Comput. Phys. Commun. **197**, 239 (2015).

[54] C. Degrande, C. Duhr, B. Fuks, D. Grellscheid, O. Mattelaer, and T. Reiter, Comput. Phys. Commun. **183**, 1201 (2012).

[55] V. Hirschi, R. Frederix, S. Frixione, M. V. Garzelli, F. Maltoni, and R. Pittau, J. High Energy Phys. 05 (2011) 044.

[56] G. Ossola, C. G. Papadopoulos, and R. Pittau, Nucl. Phys. **B763**, 147 (2007).

[57] G. Ossola, C. G. Papadopoulos, and R. Pittau, J. High Energy Phys. 05 (2008) 004.

[58] R. D. Ball et al., Nucl. Phys. **B867**, 244 (2013).

[59] G. Aad et al. (ATLAS Collaboration), Eur. Phys. J. C **74**, 3071 (2014).

[60] ATLAS Collaboration, Report No. ATL-PHYS-PUB-2013-004, 2013.

[61] ATLAS Collaboration, Report No. ATL-PHYS-PUB-2014-014, 2014.

[62] ATLAS Collaboration, Report No. ATLAS-CONF-2014-026, 2014.

[63] G. Cowan, K. Cranmer, E. Gross, and O. Vitells, Eur. Phys. J. C **71**, 1554 (2011); **73**, 2501(E) (2013).